

# Extruded Briquettes – New Charge Component for the Manganese Ferroalloys Production

Aitber BIZHANOV,<sup>1)\*</sup> Ivan KURUNOV,<sup>2)</sup> Gennady PODGORODETSKYI,<sup>3)</sup> Victor DASHEVSKYI<sup>4)</sup> and Alexander PAVLOV<sup>3)</sup>

1) J.C.Steele & Sons, Inc., 710 South Mulberry Street, Statesville, NC 28677 USA.

2) Novolipetsk Steel(NLMK), pl. Metallurgov 2, 398040, Lipetsk, Russia.

3) National University of Science and Technology (MISIS), Leninskiy prospect 4, 119991 Moscow, Russia.

4) Baykov Metallurgy and Materials Institute (IMET), 49, Leninskiy prospect, Moscow, 119991, Russia.

(Received on April 25, 2014; accepted on June 25, 2014)

The results of the laboratory study and the full-scale industrial testing of the extruded briquettes (BREX) application for the production of the Ferroalloys are discussed. Stiff vacuum extrusion agglomeration provides for the high metallurgical properties of the agglomerates leading to the economic attractiveness of this technology. BREX can be efficiently used as one of the essential charge component (up to 30% of the ore part of the charge) for the Silicomanganese smelting thus improving technical and economical parameters of the furnace and decreasing the self-cost of the Silicomanganese production.

KEY WORDS: extrusion briquette (BREX); stiff vacuum extrusion; manganese ore fines; Baghouse dust; coke rate; Submerged EAF; Silicomanganese; electric energy consumption; recovery.

## 1. Introduction

The stiff vacuum extrusion agglomeration technology of various anthropogenic and natural fine materials and wastes is known as an efficient method of the production of the extruded briquettes (BREX™ Russian Certificate#501182, priority 02.03.2012) with the high metallurgical properties for the ironmaking.<sup>1–6)</sup> The present paper considers the application of this technology for the production of the Manganese Ferroalloys. We have attempted to apply the stiff extrusion agglomeration technology in the industrial production of manganese ferroalloys, Silicomanganese in particular. With this we pursued the following goals:

1. To develop rational procedure to utilize the fine wastes of the ferroalloy production (Baghouse dusts) thus improving the ecological situation.
2. To reduce the self-cost of production substituting expensive lumpy manganese ore in the furnace charge by the agglomerates.
3. Explore the possibility of lowering the coke rate at the expense of carbon containing in BREX.

From the technological point of view it is unreasonable to add the manganese ore fines and aspiration dusts to the furnace charge since its gas regime and the exhaust gases pressure will remove the major part of these substances from the furnace without their participation in smelting. The addition of the non-agglomerated fine substances and dusts to the furnace charge leads to:

1. Disruption in furnace top gas permeability, hanging

and downslide of the charge, which leads to the fluctuations in the load on the furnace electrodes and finally to a loss of power.

2. Significant increase of dust formation from the gas cleaning systems.
3. Decreased recovery of the main component of the metal due to its loss in the dust.
4. Sharp increase in accident rate with the increased time of ‘hot idle’ state.
5. Deterioration of technical and economic parameters of the furnace in general and to the increase in production cost.

To overcome the above shortcomings associated with the use of non-agglomerated fines, it was decided to use BREX as a charge component for the industrial Submerged EAF.

## 2. Experimental

### 2.1. Materials

Following the mentioned above objectives, we performed laboratory study aimed at choosing of the most suitable BREX composition from the materials and wastes provided by customer-major producer of ferroalloys in West Virginia (United States). Manganese ore concentrate and furnace Baghouse dust chemical composition is given in **Table 1**. Particles size distribution of the ready mix containing 70% of the manganese ore concentrate and 30% of the furnace Baghouse dust by mass is given in the **Fig. 1**.

Coke breeze samples were also provided by the customer and had the following properties: moisture content 8.97%; ash 13.28%; volatiles 3.45%; sulphur 0.61%. Since the coke

\* Corresponding author: E-mail: abizhanov@jcsteele.com  
DOI: <http://dx.doi.org/10.2355/isijinternational.54.2206>

**Table 1.** Manganese ore concentrate chemical composition.

Substance	Manganese ore concentrate chemical composition (%)								
	Mn	MnO	Fe <sub>2</sub> O <sub>3</sub>	FeO	Al <sub>2</sub> O <sub>3</sub>	SiO <sub>2</sub>	CaO	MgO	P
Mn ore	35.0–45.0	–	1.2–2.2	–	2.0–3.5	14.0–25.0	2.0–3.5	0.86	0.20
Baghouse dust	–	29.74–31.41	–	0.30	0.01	30.0–34.0	1.67–2.42	1.50	–

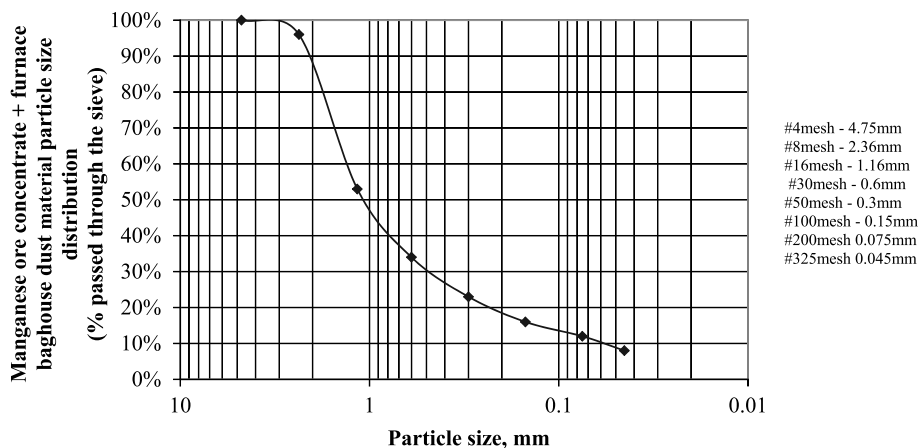


**Fig. 1.** Particles size distribution of the mix for the agglomeration by the lab-scale extruder.

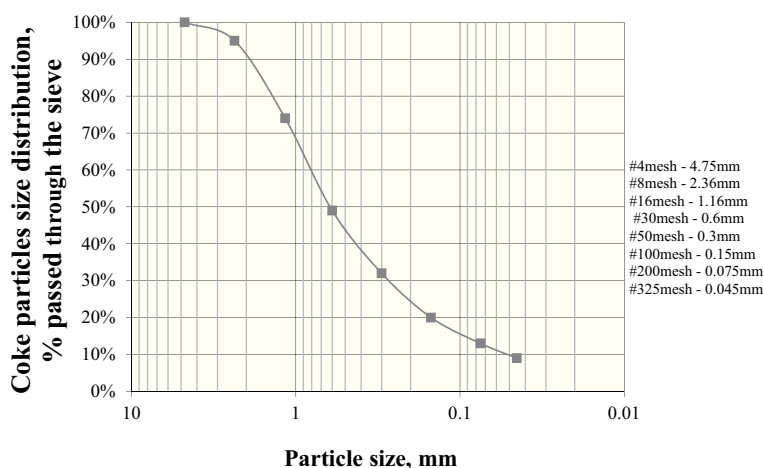


**Fig. 2.** Particles size distribution of the pulverized coke breeze.

**Table 2.** BREX components.

BREX components	BREX components (%)		
	# 1	# 2	#3
Manganese ore concentrate	47.6	66.7	56
Coke breeze	–	–	15
Baghouse dust	47.6	28.6	24
Portland cement	4.8	4.7	5

breeze was coarser than required for extrudability we pulverized it by the lab-scale smooth roll crusher. The particle size distribution of the pulverized coke breeze is shown by Fig. 2.

The following compositions of the BREX have been chosen (Table 2) and the set of the samples has been manufactured with the help of the lab-scale extruder which simulates the processing of the material through the feeder to the pug mill and then to the sealing auger and die, into the vacuum

chamber, and then the extrusion itself. We have manufactured BREX with the round cross-sections (diameter 1”; length equal to 1.5–2.0 diameters). Moisture content was measured using a moisture balance. Average moisture content of the green BREX was 11%. Vacuum applied for the production of the BREX was at the range 38–48 mm Hg.

**2.2. BREX Mechanical Strength**

Due to the cylindrical shape of the BREX we have measured both the cold compressive strength (CCS) and the tensile splitting strength since the BREX in stockpile will be subjected to these kinds of the load. These values were measured by on the Instron 3 345 device (USA). For the measurement procedure we have prepared the required amount of the specially shaped BREX samples and subjected them to the compression and tensile splitting.

The behavior of the BREX and the mechanism of their decomposition under the compressive and tensile splitting conditions are illustrated by Figs. 3 and 4. At the initial

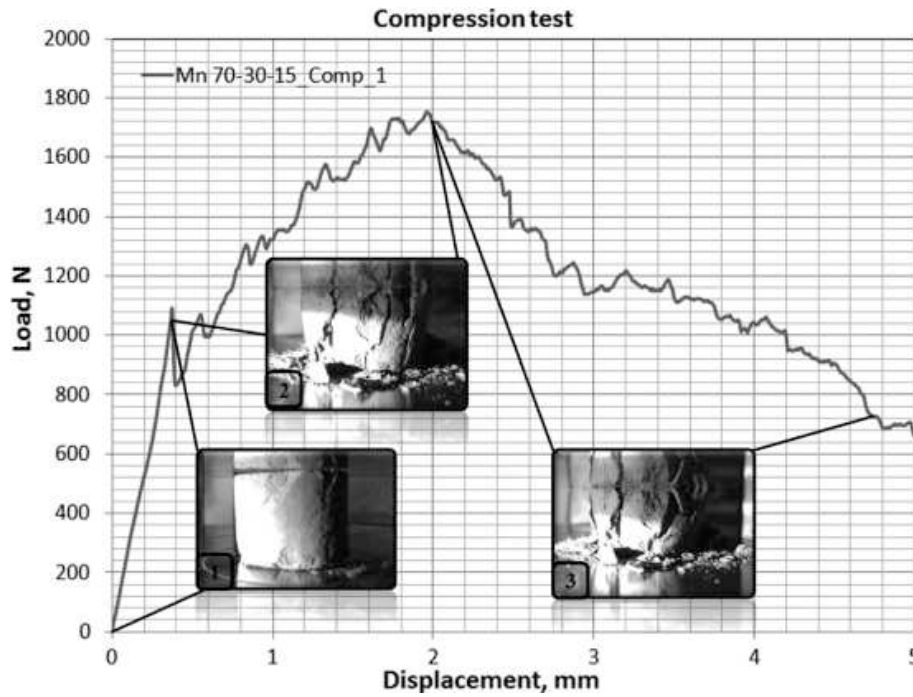


Fig. 3. Compression test of the BREX #3.

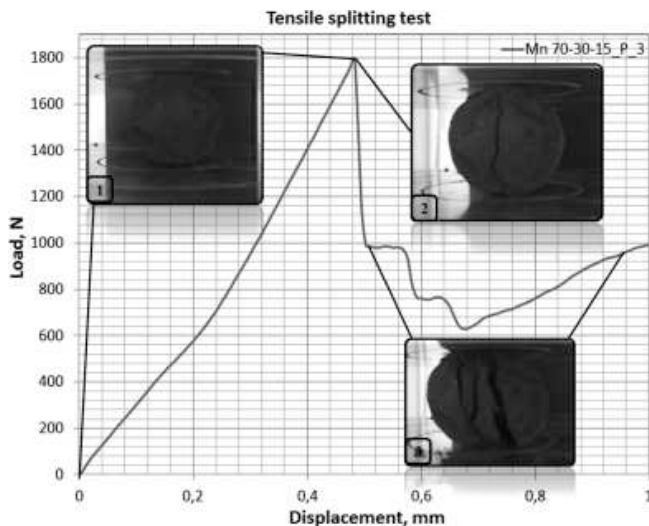


Fig. 4. Tensile splitting test of the BREX #3.

stage (1) it is observed an elastic loading of the BREX with linear dependence between current load and displacement of the active pressing surface. The beginning of the second phase is characterized by a sharp drop in load due to formation of the surface cracks. At this stage the destruction and flaking of the “near-surface” layers (15–20% of the radius) of BREX is taking place. However, the “core” (central part) of BREX continuing to perceive pressure, as evidenced by its smooth growth. There has been a pronounced zonal structure of BREX in the radial direction. And “near-surface” layers of BREX have relatively greater stiffness than the core. This is confirmed by the difference in angles of the curves on stages 1 and 2.

In step 3, after reaching the maximum of the load, the destruction of the “core” of the BREX with the complete loss of bearing capacity takes place.

The initial phase is characterized by a linear current load

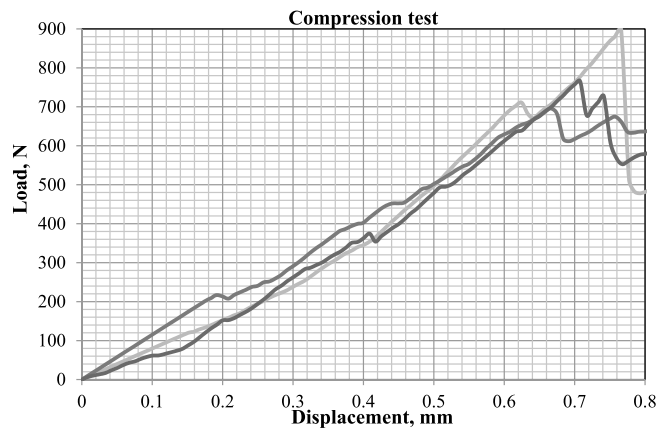


Fig. 5. Compression test of BREX #2 (for three different samples of the BREX #2).

of the vertical movement of the active pressing surface. Then the creation of the radial crack along the lines of the load application is taking place. The crack appears first in the “core” of the BREX.

Similar behavior was exhibited by BREX #1 and BREX #2. The Figs. 5 and 6 show the compressive and tensile splitting charts for the BREX #2.

The average values of the CCS and tensile splitting strength are given in Table 3.

These values refer to the specially prepared samples of the BREX with diameter 25 mm and length 20 mm. The samples of the industrial BREX #2 were tested by an independent laboratory (L. ROBERT KIMBALL & ASSOCIATES, INC., Ebensburg, Pennsylvania, USA). The CCS of BREX with diameter 32.3 mm and length 57.7 mm the CCS value was at the level of 206 kgF/cm<sup>2</sup>. One can see that these values are more than outweigh the value of CCS usually required for the Submerged EAF. And this level has been achieved by the relatively small amount of Portland cement. For the

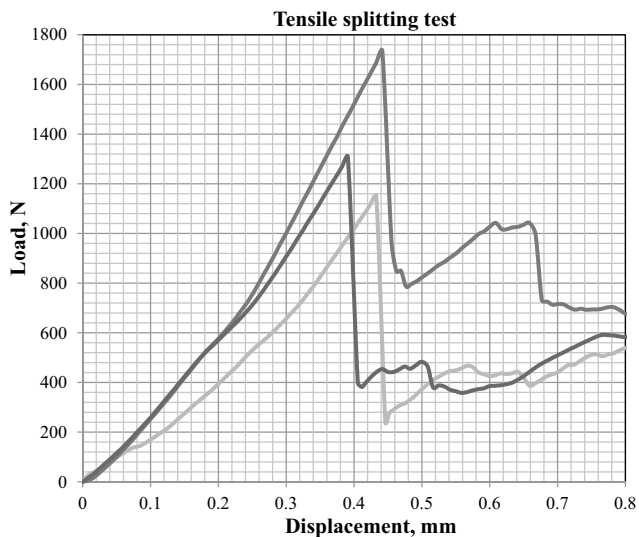


Fig. 6. Tensile splitting test of BREX #2 (for three different samples of the BREX #2).

Table 3. Mechanical strength of the experimental BREX. (kgF/cm<sup>2</sup>)

BREX #	Tensile splitting,	CCS
1	18.3	160.8
2	13.1	124.6
3	28.6	291.2

major part of 2 000 metric tons the Extruder manufactured strong BREX with only 3% of this binder. However the furnace Baghouse dust had also contributed to the strength of the BREX due to its binding properties (pozzolonic property). The difference in binder addition levels between experimental and an industrial BREX can be attributed to more thorough processing of the raw materials within the industrial extrusion line starting from the auger even feeder and then in pug mill and Pugsealer and finally in the extruder.

### 2.3. BREX Thermal Analysis

By thermal analysis, we identified the transformation that can take place in BREX when heated. Studies were performed using the STA 449 C instrument (Germany) in argon atmosphere by heating powdered samples weighing 50–70 mg in the temperature range 20–1 400°C at 20°/min.

The Fig. 7 shows that the thermal effects on the DSC curve for BREX #1 and #2 are almost identical. The mass losses have been associated mainly with the removal of constitutional water and moisture of hydrates. In general, the water content range in samples 1 and 2 has been 6–8%.

Weakly expressed endothermic effects in the temperature range of 300–450°C are due to the mass loss. This can be attributed to the reduction of MnO<sub>2</sub> to Mn<sub>2</sub>O<sub>3</sub> in accordance with the well-known equilibrium relations in Mn–O system.<sup>7)</sup> Smaller values of the temperatures of the transition in this case can be attributed to the smaller values of the O<sub>2</sub> partial pressures. In the same range, a phase dehydration of manganite (MnO(OH)) with the creation of the kurnakit (Mn<sub>2</sub>O<sub>3</sub>) occurs following the reaction: 2MnOOH = Mn<sub>2</sub>O<sub>3</sub> + H<sub>2</sub>O.

Exothermic peaks with a maximum at 795.8°C ((a) and

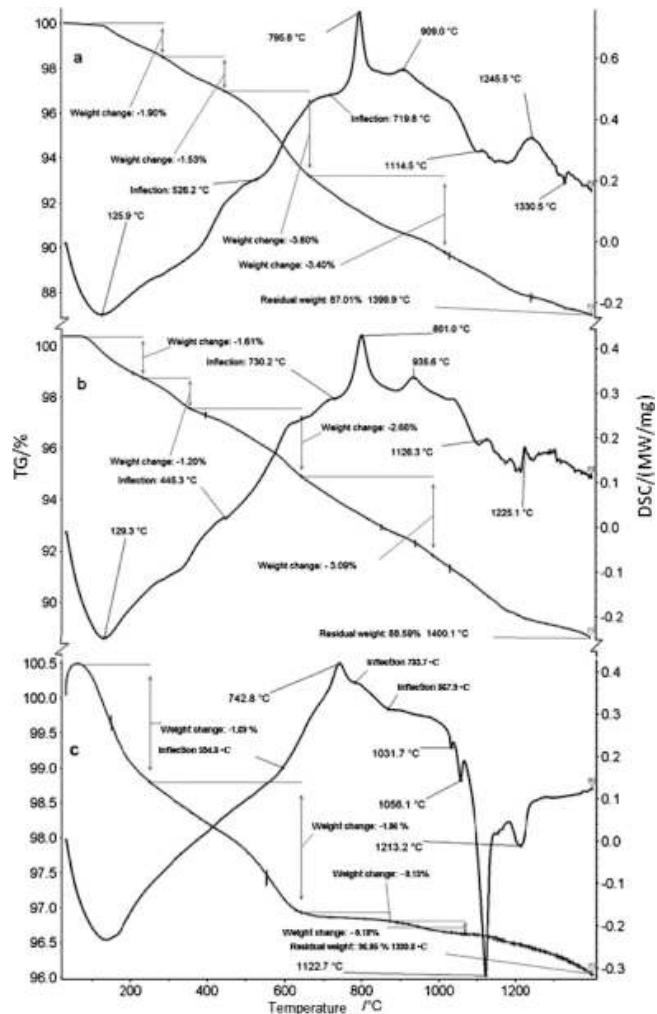


Fig. 7. Thermograms of the BREX samples #1 (a), #2 (b), #3 (c) (left hand vertical TG/%; right hand vertical-DSC/(MWt/mg).

801.0°C (b) are most likely associated with the processes of the decrystallization of the amorphous and recrystallization of the fine hydroxides of iron and manganese. At temperatures close to 800°C the pronounced exothermic effect is, probably, due to the beginning of the solid-phase interaction in the system FeO–SiO<sub>2</sub>–CaO. At temperatures above 1 000°C carbonate decomposition begins, which ends at 1 400°C.

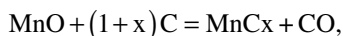
For the BREX #3 an endothermic peak in the range 150–200°C is accompanied by the mass loss of 1.69% (c). This is due to the removal of the sorption moisture from the sample. At 594.8°C (c) the DSC curve shows an inflection which is also accompanied by a loss of mass. This endothermic effect can be attributed to the effect of reduction of lower oxides of manganese to Mn<sub>3</sub>O<sub>4</sub>. The exothermic effect at 742.8°C practically not accompanied by weight loss and it can be explained by recrystallization or crystallization of amorphous phases. Effects at 783.7 and 867.9°C are also not accompanied by weight loss, so they cannot be associated with the reduction of manganese. These effects are obviously related to the iron containing phase of BREX. The endothermic effect with a maximum value reached at 1 031.7°C is associated with the reduction of Mn<sub>3</sub>O<sub>4</sub> to MnO, because it is accompanied by weight loss, and the effect at 1 056.1°C is associated with the phase change in the ferric phase. Endothermic peak with a maximum at 1 122.7°C is due to

the formation of manganese carbide  $Mn_3C$ , which recovers carbon manganese from  $MnO$ .<sup>8)</sup>

In BREX #3 the exothermic peak occurs at a lower temperature (742.8°C) and is less intensive than in BREX #1 and #2. The presence of the coke breeze in the BREX body provides for the earlier reduction of iron and manganese, which is demonstrated by the peaks at 1122.7°C and 1213.2°C.

In the presence of carbon, oxides  $MnO_2$ ,  $Mn_2O_3$  and  $Mn_3O_4$  are known to interact both with solid carbon and carbon monoxide CO. Manganese oxide MnO can be reduced by the solid carbon only. The manganese oxides inside the BREX in presence of the coke breeze will be subjected to the reduction while heating. However, this process will take place not only at the expense of solid carbon. At the same time there will be a process of oxides dissociation and recovery of higher oxides of manganese with carbon monoxide.

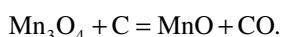
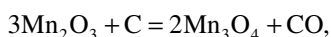
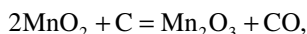
Under the temperature conditions of the real smelting the dissociation takes place till the oxide MnO, which is further reduced by the solid carbon according to the reaction:



$$\Delta G^\circ T = 196\,293 - 123T, \text{ J/mole},$$

Where  $\Delta G^\circ_T$  – Gibbs energy; T – temperature, K.

In case of close contact of manganese materials with the carbon contained inside the BREX, recovery of higher oxides may involve carbon:



Despite the close contact of the constituents influences positively on the kinetics of reduction and can lead to the increase in the manganese ore fines and coal briquettes softening temperature from 750–850°C for the manganese ore fines briquettes to 1259–1400°C for the briquettes with coal, the choice of the optimal amount of carbon in BREX should be determined based on a few important factors influencing strongly on the BREX behavior in the furnace. The presence of carbon influences on the hot strength and electrical resistivity of the BREX. Carbon burnout may increase porosity and reduced its strength during the heating. Decrease of the electric resistivity of the BREX can also lead to their instability due to the extremely high current density.<sup>9)</sup>

#### 2.4. Electric Resistivity of the BREX

Electric resistivity measurement has been implemented with the help of the specially assembled facilities based on the platform NI ELVIS II, (USA) which allows generating a voltage from –10 to 10 V, and also contains 8 differential amplifiers for voltage measurements, 24 digital I/O lines.

When measuring the resistivity of BREX, its own capacity leads to the accumulation of the charge. Thus the ohmmeter readings deviated eventually while the stationary position of the sample. To minimize the impact of this

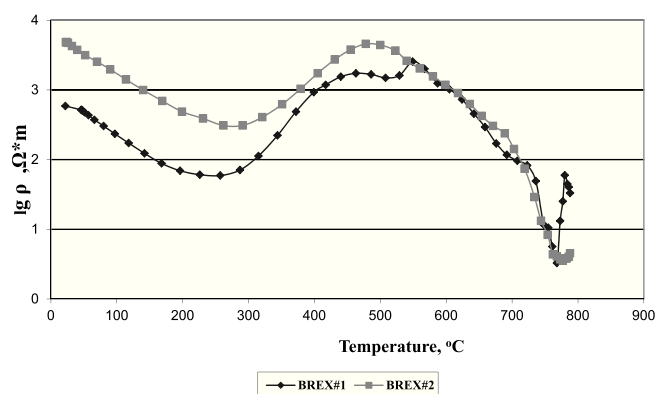


Fig. 8. Specific electric resistance of the BREX #1 and BREX #2.

capacitive component the special circuit was developed. Platform management and calculation was performed using specially written software.

It was decided to study the dependence of resistance on temperature during the heating the BREX up to 800°C, *i.e.* in the range until the first manifestations of exothermic peak. This will correspond with the sufficiently deep penetration of the BREX into the burden of the furnace.

The results of the resistivity measurements for the BREX #1 and #2 are given at Fig. 8.

The growth of the resistivity in the range of temperatures between 300 and 500°C coincides with the described above endothermic effects in the temperature range of 300–450°C caused by the mass loss which is attributed to the dehydration of manganite with the generation of kurnakit.

We can see that due to the higher carbon content brought to the BREX by baghouse dust the resistivity of the BREX #1 is lower than that of the BREX #2. We expected that this parameter for the BREX #3 will reach even lower values since the carbon will also be added by coke. We have measured the resistivity of the BREX #3 at ambient temperature and estimated it to be equal to  $1.6 \times 10^{-3}$  against  $4.8 \times 10^{-3}$  for the BREX #2. Such a low specific resistivity of the BREX #3 (sufficiently lower than that of the lumpy ore)<sup>10)</sup> will require special study of its usability in Submerged EAF. Based on these comparisons it has been decided to choose the BREX #2 for further considerations as the charge component for the full-scale trial.

#### 2.5. BREX Porosity

The important role in the BREX reduction in Submerged EAF will be played by the porosity of the agglomerate. The application of the vacuum during stiff extrusion would have resulted in the higher values of the BREX density what can be conjugated with the lower values of the porosity. To investigate this we have applied the Scanning Electronic Microscope LEO 1450 VP (Carl Zeiss, Germany) with the resolution 3.5 nm together with the X-ray high-resolution computed tomography system Phoenix V|tome|X S 240 (General Electric, USA). X-ray computed tomography has been used to detect the share of the macro pores (size larger than 100 μm). For the smaller size pores the SEM had been applied. The approach based on the STIMAN<sup>11)</sup> computer software has been used to calculate the porosity detected by SEM. The results of these measurements showed that the total porosity of the BREX #2 was equal to 18.5% (5.6%

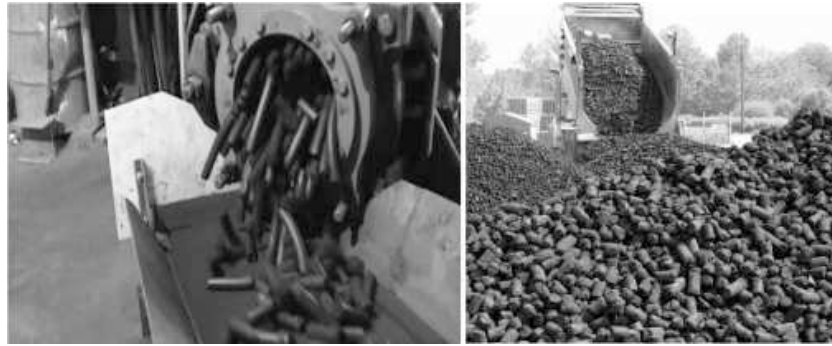


**Fig. 9.** Production of the BREX by Steele 75 Extruder (left) and discharge of the green BREX after 5–15 minutes at the storage area (right).

measured by X-ray computed tomography and 12.9% by SEM). The void ratio of the industrially produced BREX of this composition has been measured by independent laboratory (L. ROBERT KIMBALL & ASSOCIATES, INC., Ebensburg, Pennsylvania, USA) and was in the range of 0.21–0.23 corresponding with the porosity values in the range of 17.4–18.7%. We have applied the same approach for the porosity measurement of the vibropressed briquettes consisting of the manganese ore fines with 29.2% of Mn content (90%) and bonded by the 10% of the Portland cement. The porosity was equal to 15.9% (2.5% measured by X-ray computed tomography and 13.2% by SEM).

Thus the BREX #2 exhibits quite satisfactory porosity which is comparable with the porosity of some of the commercial ores<sup>9)</sup> ensuring its good reducibility.

## 2.6. BREX for Full-scale Trial Production

To manufacture a BREX batch lot of 2 000 tons the brick-making plant equipped with a J. C. Steele industrial extrusion line located in Ragland (Alabama, USA) was selected. 1 400 tons of the Manganese ore fines from the Republic of Georgia (Chiatura) and 600 tons of the Baghouse aspiration dusts from the Client's ferroalloys plant in West Virginia were delivered for the BREX production. The production process in the brick-making plant consisted of blending the dust and ore volumetrically via front end loader into blending stockpiles. Because the ore came in coarser than was desirable, the material blend was fed into the plant through the grinding facility where the material was reduced to minus 8 mesh (2.25 mm). The blended and ground material was transferred into the feed tanks in the extrusion plant. The blend was further fed into Steele 75ADC Extruder where it was mixed with water and 3%–5% of PC. The extruder and its vacuum mixer had a combined 338 KW capacity. The Extruder was equipped with multi-hole extrusion die with round openings of 25 & 30 mm diameter. Typical production parameters were as follows: production rate 55 metric tons per hour; moisture content of the green BREX 10.5%; vacuum level: 100 mm Hg. The appearance of the BREX on the outlet of the extruder and in the storage area after just 5–15 minutes after production is shown in **Fig. 9**. One can see that on leaving the extruder the BREX are very long (up to 10 diameters in length). At the same time, the average length of BREX in the storage area does not exceed 2.5 diameters. The decomposition of the elongated BREX during transportation by conveyors and discharge

on the floor was described by Bizhanov *et al.*<sup>6)</sup> The reason for this is the bending of the elongated BREX due to its gravity at the exit from the extruder that resulted in generation of 2–3 concentrators of the strain in the areas of the future decomposition of this BREX.

As expected, the green BREX handling procedure did not require any special protective measures or special treatment (steam curing, palletizing to preserve the integrity, *etc.*). The BREX were shipped to the smelter by barges and were discharged at the berth of the Ohio River. Transportation from the pier to the open batch stockyard was made by trucks, followed by a conveyor directly to the furnace bunkers. In total the transportation of the BREX to the ferroalloy (2 000 km) withstood 20 handling operations during 30 days: manufacturer → extruder, conveyors, dumps truck, stockpiles, wheel loader, truck; port of loading → stockpiles, wheel loader, hopper, bucket, barge; port of discharge → grab, hopper, conveyors, truck; ferroalloy plant ore storage yard → stockpiles, front loader, factory warehouse, furnace. Total fines generation during these operations (less than 6 mm) did not exceed 10%.

## 3. Full-scale Trial at Ferroalloys Smelter

To initiate a full-scale industrial trial, a stable 27MVA-capacity and 85-tons/day-average production industrial Submerged EAF was selected to run with the specific average energy consumption at 4 200 kWh/t, manganese recovery rate at 80%, and manganese content of the dump slag at 12–14%. The chemical composition of manganese containing charge components is shown in **Table 4**.

Scraps are the internal wastes generated while deslagging of the surface of the metal in the ladle, cleaning buckets and furnace notch, sorting at the slag dumps, and casting of Silicomanganese. Only the total content of manganese in slags was determined and these values are given in **Table 5**. Briquettes made from Silicomanganese fines are produced by vibropressing process (unconditioned fines fraction 0–6 mm). To impart the necessary strength to the briquettes made from these fines, significantly more Portland cement was required than for BREX (10%).

A preliminary calculation of the charge composition was made in order to achieve stable manganese content in the ore part of the charge (**Table 6**). With the increase in the share of BREX in the ore part of the charge, it was decided to reduce the supply of ore-2, which is a drop-in replace-

ment, because the average manganese content of BREX was 31% against 29% in the said grade.

For the correctness of the comparison of the results of the furnace operation with and without BREX, a month-long period of the furnace operation was taken. A weeklong period of work of the furnace without BREX immediately preceding the beginning of the pilot operating period was chosen as the reference.

**Table 4.** The chemical composition of the charge components.

Material	Components composition (%)						
	Mn	SiO <sub>2</sub>	CaO	MgO	Al <sub>2</sub> O <sub>3</sub>	Fe	P
Ore-1	49.5	13.0	0.7	0.5	1.0	4.0	0.05
Ore-2	29.0	20.2	5.9	5.2	2.1	0.9	0.06
BREX	31.37	24.32	6.10	2.05	2.79	1.36	0.12
Scraps	23.3–38.6	N/A	N/A	N/A	N/A	N/A	N/A
Silicomanganese fines Briquettes	53	18	4	N/A	N/A	10.5	0.15

**Table 5.** Basic element content in metal and slag.

BREX share, %	Basic elements content, % mass									
	in metal				in slag					
	Mn	Si	Fe	P	MnO	MgO	SiO <sub>2</sub>	CaO	Al <sub>2</sub> O <sub>3</sub>	
0	66.64	17.71	14.06	0.127	10.50	7.38	44.28	21.43	15.29	
5	66.33	16.30	14.25	0.128	12.70	7.14	45.33	20.31	13.46	
10	66.90	17.69	14.18	0.098	12.89	6.52	44.78	18.67	13.80	
20	66.77	16.45	14.21	0.12	11.30	6.77	44.57	19.86	15.07	
29	68.02	16.02	14.01	0.14	11.79	6.39	45.11	19.42	15.13	
35	65.98	15.22	14.30	0.16	15.08	5.73	46.20	26.11	15.71	
40	66.08	17.07	14.25	0.18	10.8	5.17	45.30	19.83	15.35	

It was decided to begin with 5% of the BREX share in the ore part of the charge to get a first experience with the agglomerated burden. During the three days of observation no visible changes in the process of Silicomanganese smelting had been registered, the furnace worked smoothly, with a constant and uniform current load during the period of use of BREX. The slight decrease in manganese extraction by 0.3% during this period was due to the furnace downtime associated with the tap-hole unit repair (1.5 hours downtime).

Then, for four consecutive days, the BREX share in the charge was maintained at 10%. Improvement in the furnace top functioning was visually apparent. Gas flames throughout the furnace top area confirmed the improvement in gas permeability of the column of the charge and the uniformity of the temperature distribution over the surface of the furnace top. Deeply submerged electrodes functioned without producing surface blowholes in the electrodes circle and in the surrounding area. No sintering in the electrodes circle was observed.

During the next three days, BREX share in the charge was increased up to 20%. The furnace operated smoothly, electrodes were deeply submerged, current load had no visible abnormalities or tremors, and the gas permeability of the charge was good for the entire area of the furnace top.

Throughout the next week, the BREX share of the charge was increased to 29%. The furnace worked fine. An increase in the rate of the charge descent in the area of electrodes circle, especially during the tapping, indicates the increase in the melting rate of the charge in the active zone of the furnace. The furnace top functioned smoothly without surface blowholes with a constant load current, smooth, without bumps and drops. Melt out was good, metal and slag were sufficiently warmed up. However, in the end of this period, there was a furnace downtime for 4 hours due to reasons not related with the BREX presence in the charge (electrical problem in the transformer).

**Table 6.** Composition of the charge (net tons).

Component of the charge	Reference and Full scale trial periods						
	Reference period	1	2	3	4	5	6
Mn Ore-1	0.526 (30%)	0.525 (30%)	0.525 (30%)	0.525 (30%)	0.525 (30%)	0.525 (30%)	0.525 (30%)
Mn Ore-2	1.205 (70%)	1.12 (65%)	1.03 (60%)	0.855 (50%)	0.705 (41%)	0.6 (35%)	0.525 (30%)
BREX	–	0.087 (5%)	0.175 (10%)	0.35 (20%)	0.5 (29%)	0.605 (35%)	0.69 (40%)
Estimated weight of charge	1.73	1.732	1.73	1.73	1.73	1.73	1.74
Incoming manganese with:							
Ore-1	0.262 (43%)	0.262 (42.6%)	0.262 (42.6%)	0.262 (42.4%)	0.262 (42.2%)	0.262 (42.1%)	0.262 (41.8%)
Ore-2	0.35 (57%)	0.325 (53%)	0.299 (48.6%)	0.224 (40.1%)	0.205 (32.8%)	0.174 (27.9%)	0.152 (24.2%)
BREX	–	0.027 (4.4%)	0.054 (8.8%)	0.109 (17.5%)	0.16 (25%)	0.188 (30%)	0.214 (34%)
Manganese charge weight	0.612	0.614	0.614	0.619	0.622	0.624	0.628
Average manganese content, %	35.4	35.5	35.6	35.8	36	36.1	36.1

**Table 7.** Furnace parameters during the reference and the full-scale trial period.

Parameter		Reference and Full scale trial periods						
		Reference period	1	2	3	4	5	6
Actual metal production over a period of time, t	ton	816.323	298.4	277.1	196.6	570.6	397.2	757.2
	b.t (basic ton)	839.670	300.7	285.8	199.5	584.75	393.2	767.8
Actual furnace performance, %		98.9	97.6	97.4	99.7	96.2	98.6	93.6
Power consumption, MW		3 339.27	1 078.2	1 085.4	734.7	2 120.8	1 536.3	2 821.48
Specific power consumption, kW*h/b.t		3 977	3 586	3 798	3 682	3 627	3 908	3 675
Ore-2	t (29%Mn)/b.t	1.106	0.933	0.892	0.714	0.635	0.626	0.492
	t (48%Mn)/b.t	0.668	0.563	0.539	0.431	0.383	0.378	0.297
Ore-1	t (49.5%Mn)/b.t	0.565	0.505	0.482	0.509	0.480	0.524	0.484
	t (48%Mn)/b.t	0.582	0.520	0.497	0.525	0.495	0.540	0.499
BREX	t (31.37%Mn)/b.t	0	0.077	0.164	0.273	0.387	0.571	0.605
	t (48%Mn)/b.t	0	0.050	0.107	0.178	0.252	0.373	0.395
The total consumption of raw manganese ore	t/b.t	1.671	1.515	1.538	1.496	1.502	1.721	1.581
	t (48%Mn)/b.t	1.250	1.133	1.143	1.134	1.130	1.291	1.191
Coke, t/b.t		0.446	0.339	0.420	0.405	0.395	0.415	0.413
Quartzite, t/b.t		0.419	0.499	0.524	0.465	0.529	0.456	0.475
Silicomanganese fines Briquettes t/b.t		0.158	0.082	0.103	0.092	0.120	0.110	0.094
Scrap (Mn content in scrap,%), t/b.t		0.358 (23.3)	0.601 (29.9)	0.462 (33.0)	0.477 (35.3)	0.461 (32.0)	0.455 (25.8)	0.373 (38.6)
Electrode mass, t/b.t		0.034	0.032	0.030	0.035	0.028	0.033	0.028
Manganese extraction from the ore component, %		80.1	79.8	80.7	80.7	83.6	79.1	79.9

The beginning of the next phase of the pilot operational period, when the BREX share rose to 35% substituting the ore-2, was associated with a problem caused by a disruption in the tap-hole electrode bypass, resulting in its shortening and the deterioration of the melt. The bulk of the slag remained in the furnace. This resulted in an increased coke rate and scraps withdrawal from the charge along with briquettes of Silicomanganese fines. During this period, a deterioration in the technical and economic performance of the furnace had been registered, namely an increase in specific energy consumption and specific consumption of manganese ore raw materials as well as a reduced extraction of manganese. To restore its normal functioning, the furnace heating rate was increased in order to warm up the slag ensuring its normal tapping.

In the final phase (week) of the pilot operation period, the furnace worked with the BREX share in the charge up to 40%. The furnace operation was characterized by a good current load, top gas release was smooth, with no surface blowholes and furnace charge downsides, and with a normal tapping.

#### 4. Results and Discussions

Based on the results of the full-scale trial, we made a comparative analysis of the technical and economic performance of the furnace with and without the BREX in the charge. Technical and economic performance of the furnace and the chemical analysis of the fusion products are presented in **Tables 7** and **8**. All the numbers are taken from the foundry journals recordings.

**Table 8.** Main components composition during the reference and pilot operation period.

Phase	Main components composition (%)									
	in metal				in furnace charge					
	Mn	Si	Fe	P	MnO	MgO	SiO <sub>2</sub>	CaO	Al <sub>2</sub> O <sub>3</sub>	
Reference	66.64	17.71	14.06	0.127	10.50	7.38	44.28	21.43	15.29	
1	66.33	16.30	14.25	0.128	12.70	7.14	45.33	20.31	13.46	
2	66.90	17.69	14.18	0.098	12.89	6.52	44.78	18.67	13.80	
3	66.77	16.45	14.21	0.12	11.30	6.77	44.57	19.86	15.07	
4	68.02	16.02	14.01	0.14	11.79	6.39	45.11	19.42	15.13	
5	65.98	15.22	14.30	0.16	15.08	5.73	46.20	26.11	15.71	
6	66.08	17.07	14.25	0.18	10.8	5.17	45.30	19.83	15.35	

The main positive aspect of the full-scale campaign with the BREX in the charge for the smelting of merchandise Silicomanganese is that the furnace operated in a stable, smooth regime. Furnace top operation was characterized by good gas permeability all over the surface, without any charge downslide. Current load was uniformly distributed among three electrodes. Electrodes were submerged deeply and stable. Melt tapping took place according to the schedule, the chemical composition of the metal and slag showed no significant changes. Replacement of the substantial part of the lumpy manganese ore by BREX based on ore fines and aspiration dust led to the improvement of technical and economic indicators of the process as a whole.

Specific energy consumption during the test period decreased significantly. In the reference period, consumption per basic ton of the alloy was 3 977 kWh. With the BREX share in the ore part of the charge equal to 40% the specific energy consumption decreased up to 3 675 kWh per basic ton (−7.6%).

Another positive result of the full-scale trial is related with the increased manganese extraction from the ore. With the 29% of BREX in the ore part of the charge the manganese extraction was 83.6% against the average extraction of 80% in the reference period of the furnace operation without BREX in the charge (see Fig. 10). Decreased extraction in the period preceding the final phase was not associated with the presence of BREX in charge and was the result of furnace downtime and problems with the electrode.

It is also important to know the relationship of the BREX share in the ore part of the charge with the specific productivity of the furnace expressed in base tons per unit of electricity consumed. The Fig. 11 shows that the best performance is achieved when the BREX share in the ore part of the charge is in the range of 20 to 30%.

In general the results of the full-scale trials give grounds to consider that it is appropriate to use BREX based on man-

ganese ore fines and baghouse dust from gas-cleaning as the essential charge component for the Silicomanganese smelting.

## 5. Conclusions

From the results obtained it follows that:

- (1) Manganese ore concentrate and the Baghouse dust can be efficiently agglomerated by the stiff vacuum extrusion technology.
- (2) BREX have sufficient mechanical strength to withstand the distant transportation including multiple loading-discharging operations. Mechanical strength of the BREX is significantly higher even with addition of relatively small amount of the Portland cement binder than the strength requirements to the charge components of the Submerged EAF. Furnace Baghouse dust is also exhibiting binder properties. Increase of Baghouse dust content over 30% reduces mechanical strength of briquette.
- (3) BREX have sufficient porosity to ensure their good reducibility. The porosity level is comparable with that of commercial manganese ores.
- (4) BREX exhibit high thermal stability and sufficient hot strength ensuring the stable and smooth operation of the furnace.
- (5) BREX with the Baghouse dust content up to 30% will exhibit sufficient specific electric resistivity comparable with the specific electric conductivity the lumpy ores.
- (6) BREX can be efficiently used as one of the essential charge component (up to 30% of the ore part of the charge) for the Silicomanganese smelting thus improving technical and economical parameters of the furnace and decreasing the self-cost of the Silicomanganese production.

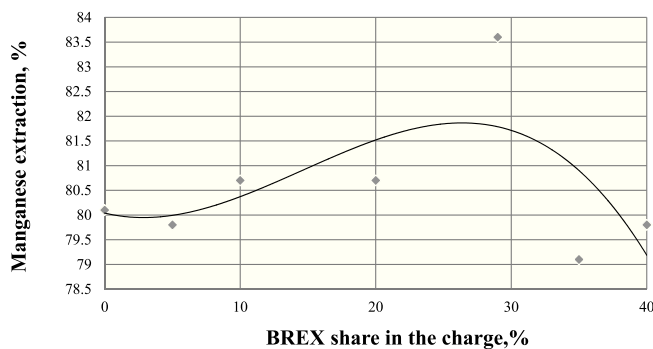


Fig. 10. Manganese extraction as a function of the BREX share in the ore component in the furnace charge.

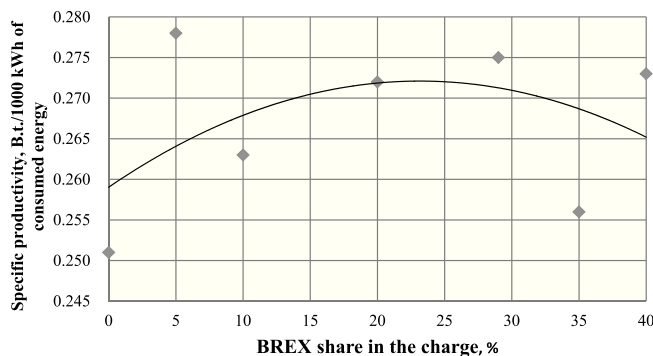


Fig. 11. Specific productivity, B.t./1 000 kWh of consumed energy.

## REFERENCES

- 1) Y. K. Dalmia, I. F. Kurunov, R. B. Steele and A. M. Bizhanov: *Metallurgist*, **56** (2012), 164.
- 2) I. F. Kurunov, A. M. Bizhanov, D. N. Tikhonov and N. R. Mansurova: *Metallurgist*, **56** (2012), 430.
- 3) A. M. Bizhanov, I. F. Kurunov, N. M. Durov, D. V. Nushtaev and S. A. Ryzhov: *Metallurgist*, **56** (2012), 489.
- 4) A. M. Bizhanov, I. F. Kurunov, N. M. Durov, D. V. Nushtaev and S. A. Ryzhov: *Metallurgist*, **56** (2013), 736.
- 5) A. M. Bizhanov, I. F. Kurunov and D. V. Ivonin: *Metallurgist*, **57** (2013), 579.
- 6) A. M. Bizhanov, A. Pavlov, O. Chadaeva, Y. Dalmia and B. Mishra: *ISIJ Int.*, **54** (2014), No. 6, 1450.
- 7) Sverre E. Olsen, Merete Tangstad and Tor Lindstad: Production of Manganese Ferroalloys, Tapir Academic Press, Sweden, (2007), 247.
- 8) E. F. Vegman, B. N. Zhrebina, A. N. Pokhvisnev, Y. S. Yusfin, I. F. Kurunov, A. E. Parenkov and P. I. Chernousov: *Metallurgy of Cast Iron*, Akademkniga, Moscow, Russia, (2004), 774.
- 9) M. I. Gasik, N. P. Lyakishev and B. I. Emlin: *Theory and Technology of the Production of the Ferro Alloys*, Metallurgiya, Moscow, (1988), 784.
- 10) A. V. Zhdanov, O. V. Zayakin and V. I. Zhuchkov: *Electrometallurgy*, **6** (2007), 24.
- 11) V. N. Sokolov, D. I. Yurkovets, V. N. Melnik, A. Boyde and P. G. T Howell: Proc. of Inst. of Physics Electron Microscopy and Analysis Group Conf., Institute of Physics Publishing, Bristol, Philadelphia, (2001), 119.